Atmospheric Pollution Research 17 (2026) 102768

Contents lists available at ScienceDirect

Atmospheric Pollution Research

journal homepage: www.elsevier.com/locate/apr

Ozone effects in coffee (*Coffea arabica* L.) plants: Cultivar-specific responses and risk assessment

Barbara Baesso Moura [a,b], Marisa Domingos [c], Emerson Alves da Silva [c], Jacopo Manzini [a,d], Elena Marra [a], Leonardo Lazzara [a], Rodrigo Fazani Esteves Sanches [c], Elena Paoletti [a,b], Yasutomo Hoshika [a,b,*]

[a] *Institute of Research on Terrestrial Ecosystems (IRET), National Research Council of Italy (CNR), Via Madonna del Piano 10, 50019 Sesto Fiorentino, Italy*
[b] *National Biodiversity Future Center (NBFC), Palermo 90133, Italy*
[c] *Instituto de Pesquisas Ambientais (IPA), Caixa Postal 68041, 04045-972 Sao Paulo, Brazil*
[d] *Department of Agriculture, Food, Environment and Forestry (DAGRI), University of Florence, Piazzale delle Cascine, 18, 50144, Firenze, Italy*

ARTICLE INFO

Keywords:
Tropospheric ozone
Coffee cultivars
Dose-response relationship
Stomatal conductance
Critical levels

ABSTRACT

The environmental sustainability of agricultural production faces critical challenges due to climate change, with tropospheric ozone (O_3) being a significant concern. This study investigates the dose-response (DR) relationship between O_3 exposure and leaf biomass (LB, as a proxy of coffee production) reduction in three coffee cultivars (*Coffea arabica* L. cv. Geisha, IAC99, and IAC62) using both exposure- (AOT40) and flux-based (POD_Y) indices. Experiments were conducted in a Free-Air Controlled Exposure (FACE), where plants were exposed to ambient air (AA), 1.5 × AA, and 2.0 × AA O_3 levels. The study reports the O_3 visible foliar injury (O_3_VFI) on *C. arabica* leaves for the first time. It also reveals that O_3 significantly reduced total LB in the Geisha and IAC62 cultivars compared to the less affected IAC99. The stomatal conductance model was parametrized to estimate stomatal O_3 uptake and understand each cultivar's physiological response to O_3 stress. The Geisha and IAC62 cultivars exhibited higher stomatal O_3 uptake due to relatively high maximum stomatal conductance (g_{max}) values compared to IAC99, leading to greater biomass loss under elevated O_3 conditions. The DR analysis identified $POD_{1.5}$ as the most appropriate index for assessing critical O_3 levels (CLs) for LB losses. Linear regression was suitable for representing the DR relationships, and the O_3 CL for a 4 % and 10 % LB reduction was estimated at 0.29 and 0.73 mmol m^{-2} $POD_{1.5}$, respectively. These findings underscore the necessity of cultivar-specific studies for accurate O_3 risk assessment and management in coffee production.

1. Introduction

With the intensifying effects of climate change, ensuring the environmental sustainability of agricultural production has become one of the most pressing global challenges. Various climate-related factors, such as elevated temperatures, changing precipitation patterns, and increased pollution levels, may significantly reduce the yield and quality of key agricultural products (Hertel, 2016). Among pollutants, tropospheric ozone (O_3) stands out as the third most important greenhouse gas after carbon dioxide (CO_2) and methane (CH_4). Since the 19th century, background O_3 concentrations have considerably increased (Mills et al., 2018; Vazquez Santiago et al., 2024), which has raised concerns about its impact on agroecosystems (Kobayashi, 2022). Ozone contributes to the formation of reactive oxygen species (ROS), leading to oxidative stress in plants, which in turn disrupts plant physiology and biochemistry, ultimately reducing agricultural productivity (Agrawal et al., 2021). The current levels of O_3 pollution may decrease global crop yields for essential food sources such as soybean, wheat, rice, and maize, resulting in significant economic losses (Singh et al., 2018), with estimates reaching \$63 billion in Asian countries alone (Feng et al., 2022).

In particular, tropical and subtropical regions are experiencing a continuous increase in emissions of O_3 precursors such as nitrogen oxides (NO_x) due to factors like rapid population growth, urbanization, and biomass burning associated with land use changes (Miyazaki et al., 2017). Tropical regions have recorded ambient O_3 concentrations considered toxic to people and vegetation in Asia (Sicard, 2021) and

* Corresponding author. Institute of Research on Terrestrial Ecosystems (IRET), National Research Council of Italy (CNR), Via Madonna del Piano 10, 50019 Sesto Fiorentino, Italy.
E-mail address: yasutomo.hoshika@cnr.it (Y. Hoshika).

https://doi.org/10.1016/j.apr.2025.102768
Received 12 March 2025; Received in revised form 23 September 2025; Accepted 25 September 2025
Available online 26 September 2025

confirmed as the main factor for the development of O_3 visible foliar injury (O_3_VFI) observed in natural vegetation in Brazil (Moura et al., 2014). For instance, in a major tropical agricultural zone in South America, Cheesman et al. (2023) estimated a reduction in net primary production (NPP) of up to 15 % in sugarcane due to ambient O_3 exposure.

Coffee (*Coffea arabica* L.), a perennial tropical tree crop, is one of the world's most traded commodities, with Brazil being the largest global producer for over a century, with *C. arabica* corresponding to 80 % of the production and occupying around 1.82 million hectares, mainly concentrated in the southeastern region, which offers optimal edapho-climatic conditions for coffee cultivation (Conab, 2024). Although there has been extensive research on the response of coffee plants to elevated CO_2 (Sanches et al., 2020), drought (DaMatta and Ramalho, 2006; Menezes-Silva et al., 2017), and high temperatures (DaMatta and Ramalho, 2006; Rodrigues et al., 2018), there is a noticeable gap in scientific understanding regarding the impact of elevated O_3 levels on *C. arabica*.

Establishing an accurate dose-response (DR) relationship is essential for assessing the risks of O_3 to coffee production and for informing effective policy decisions (Kobayashi, 2022). Traditionally, O_3 impacts on crops have been evaluated using the Accumulated Exposure Over Threshold of 40 ppb (AOT40) index. However, a more refined approach focuses on the Phytotoxic Ozone Dose above a threshold of Y nmol m^{-2} s^{-1} (POD_Y), which is based on the actual stomatal uptake of O_3 (CLRTAP, 2017). This is because O_3 enters the plant via stomata to cause physiological damage. The estimation of stomatal O_3 uptake requires numerical models such as the DO_3SE (Deposition of O_3 for Stomatal Exchange) model, which has been recommended by the Manual on Methodologies and Criteria for Modelling and Mapping Critical Loads and Levels and Air Pollution Effects, Risks, and Trends (CLRTAP, 2017).

Despite the importance of the O_3 uptake approach in calculating DR, the DO_3SE model has not been significantly parameterized for tropical crops e.g., coffee plants. The DR relationships used to calculate critical O_3 exposure levels have usually relied on linear regression models (Hoshika et al., 2018). However, it is essential to evaluate whether nonlinear regression could provide a better fit for these relationships, particularly when linear models fail to achieve statistical significance (Hoshika et al., 2024a,b).

The objective of this study was to examine the impact of O_3 exposure on the growth of *C. arabica*, focusing on its potential to induce O_3_VFI and impairment of biomass development. Additionally, we aimed to establish the DR relationship for *C. arabica* biomass in response to O_3 exposure, using both exposure- (AOT40) and flux-based (POD_Y) indices in a Free-Air Controlled Exposure (FACE) experiment. Leaf biomass (LB) was selected as the target biomass parameter due to its known correlation with coffee yield (Bernardes et al., 2012; Abreu Júnior et al., 2022). Three different *C. arabica* cultivars with distinct drought tolerance and productivity were used in this research. The plantations found in Brazil are generally quite heterogeneous in relation to vigor, grain size, and quality of the drink, and plants are quite sensitive to drought. The IAC62 cultivar was chosen because it is the most widely grown cultivar of the Catuaí Amarelo group in Brazil, and it produces the highest quality beverage, being cultivated in various high-altitude coffee-growing regions. The IAC99 cultivar was selected due to its wide adaptability to different soil and climate conditions, including regions with high temperatures and droughts such as the Cerrado (Braun et al., 2010). Furthermore, the cultivar Geisha was chosen because it is an African cultivar recognized for its unique aromas and flavors that achieve high prices in the specialty coffee markets (Medrano et al., 2025), for presenting excellent quality.

Given coffee plants' high water use efficiency (WUE) due to low transpiration rates (Silva et al., 2004), we hypothesized that cultivars with lower stomatal conductance (g_s) might be more resistant to O_3, as limited stomatal uptake could reduce O_3-induced damage. Additionally, we explored linear and nonlinear regression models to calculate DR relationships to predict O_3 impacts on coffee growth and support risk assessments for future policy development.

2. Materials and methods

2.1. Experimental site and plant materials

Experiments were conducted at the Free-air O_3 eXposure (FO_3X) facility located at the CNR (National Research Council of Italy) experimental garden in Sesto Fiorentino, central Italy (coordinates: 43°48′49″ N, 11°12′01″ E, elevation: 55 m above sea level). Further information regarding the fumigation system is available in Paoletti et al. (2017). In this study, three *Coffea arabica* cultivars were analyzed: the Geisha cultivar (moderately drought-tolerant) was studied in 2022, while the IAC62 (drought-sensitive) and IAC99 cultivars (drought-tolerant) were studied in 2023. In December 2021, Geisha plants were obtained from a European nursery (Holland, by De Groot Nursery) and grown in a controlled environment room (Temperature [T]: 25 °C, photosynthetic photon flux density [PPFD]: 500 μmol m^{-2} s^{-1}) until spring. In May 2022, seedlings were transplanted into 5 L plastic pots filled with a 1:1:1 mixture of sand, peat, and soil and placed in the CNR experimental garden until the fumigation began. From 27th June to August 16, 2022, they were subjected to three O_3 levels, i.e., ambient (AA), 1.5 × AA (× 1.5), and 2.0 × AA (× 2.0), in the FO_3X. Each O_3 level had three replicated plots with three seedlings, totaling 27 plants (3 replicated plots × 3 plants per plot × 3 O_3 treatments).

Seeds of *Coffea arabica* L. (cv. IAC62 and cv. IAC99) were sown in February 2022 and grown in a controlled environment room (T: 25 °C, PPFD: 500 μmol m^{-2} s^{-1}) until spring 2023. One-year-old plants were thus moved to the CNR experimental garden in mid-May 2023, and the fumigation started on June 12, 2023. Plants were exposed to two O_3 levels, i.e., AA and × 2.0, for 70 days (until August 21, 2023) in the FO_3X facility ($n = 3$ plots, in total 36 plants = 3 replicated plots × 3 plants per plot × 2 O_3 treatments × 2 cultivars).

Plants of each cultivar were in optimal health status before O_3 fumigation. A drip point irrigation system provided water for all plants daily to maintain well-watered conditions. Fig. 1 represents the trend of climatic parameters and O_3 levels during both years of the experiment, The mean O_3 concentrations for AA, × 1.5, and × 2.0 treatments were 24.0 %, 32.3 %, and 32.9 % higher in 2022 (46.97, 68.23, and 94.26 ppb, respectively) than in 2023 (37.87, 51.57, and 70.91 ppb), but the overall gradients were maintained, with overlapping peak values and similar standard errors (Table S1). Meteorological parameters also differed, with PAR, mean air temperature, and VPD being 3 %, 7 %, and 33 % higher in 2022 (1535.06 μmol m^{-2} s^{-1}, 28.16 °C, and 2.32 kPa) than in 2023 (1490.95 μmol m^{-2} s^{-1}, 26.23 °C, and 1.74 kPa). Despite these variations, environmental conditions and O_3 trends were consistent across years (Fig. 1), allowing reliable comparisons of O_3 effects.

2.2. Assessment of biomass and O_3 visible foliar injury (O_3_VFI)

In each experiment (2022 and 2023), dry leaf biomass (LB) production was assessed as the parameter for measuring biomass loss. At the end of the experiments, leaves were collected and dried at 80 °C until a constant weight was achieved. In order to assess dry LB production, an extra set of plants ($n = 6$ plants) was harvested to determine the dry LB at the beginning of the experiment (in May 2022 for Geisha cultivars and May 2023 for IAC62 and IAC99). Subsequently, the LB production across the experiment was calculated by comparing the average biomass at the beginning (time zero) with that at the end of each experiment.

After positioning the plants inside the O_3_FACE facility, the assessment of O_3 visible foliar injury (O_3_VFI) was performed on leaves at full development within the O_3_FACE facility for Geisha, IAC62, and IAC99. For the cultivar Geisha, to quantify the interaction between photooxidative and O_3 stress, we also evaluated the development of O_3_VFI on leaves present on the plants before exposure to the enriched O_3

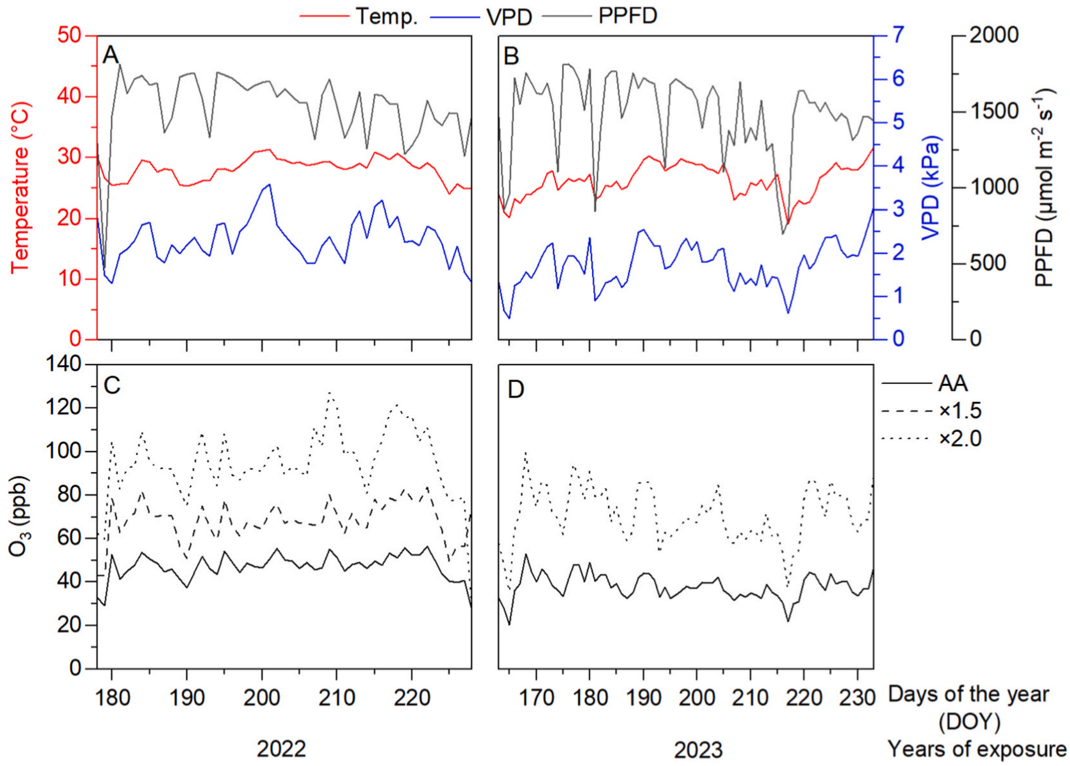

Fig. 1. Environmental conditions along the experimental periods (2022 and 2023). A) Daily average of hourly air temperature (Temperature), air vapor pressure deficit (VPD), photosynthetic photon flux density (PPFD). B) 24 h daily average O_3 concentrations at ambient (AA), 1.5 times ambient (× 1.5 – only for 2022), and twice ambient (× 2.0) O_3 treatment.

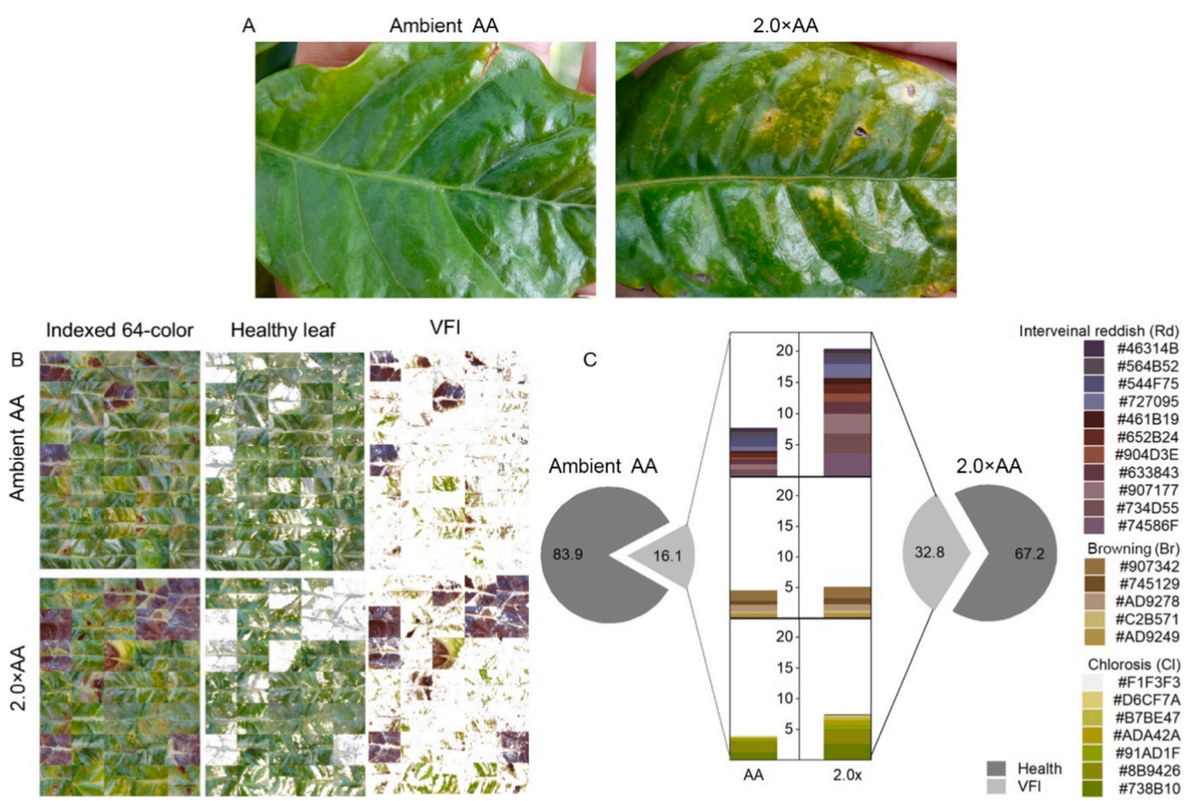

Fig. 2. Visible foliar injury (O3_VFI) on *Coffea arabica* cultivar (Geisha) leaves under different O_3 treatments. A) Ambient (AA) with no injury and 2.0 × AA O_3 treatment with chlorotic spots. B) Image analysis workflow showing indexed 64-color images, separation of healthy tissue (green) and O3_VFI categories (reddening, browning, and chlorosis). C) Quantification of O3_VFI distribution between AA and 2.0 × AA treatments.

environment, as we observed a photooxidative response in the leaves just after the exposure. We applied image analysis to 35 randomly selected leaf pictures from AA and × 2.0 treatments (a total of 70 pictures). The central regions of each leaf were captured using a digital camera (Sony Cyber-shot DSC-H300) under natural lighting conditions, following the methods of Moura et al. (2020, 2023).

All images were then compiled and merged into a single RGB figure. This merged figure was transformed using Indexed Color mode with Local (Perceptual) settings, generating a 64-color image. Thirty-eight colors represented healthy tissue, and 26 were most indicative of oxidative stress. These 26 colors were grouped into three categories: 11 related to reddening, 5 to browning, and 7 to chlorosis. The percentage of each color in each sample was quantified using Adobe Photoshop CC 2017, and color names were verified with the Hex Dictionary (https://www.hexdictionary.com/). A pictorial overview of the method is shown in Fig. 2B.

In the second year of exposure, O_3_VFI was assessed only for IAC62 and IAC99, without evidence of photooxidative interaction.

2.3. Calculation of O_3 indices

Both exposure- (AOT40) and flux-based (POD_Y) O_3 metrics were examined throughout the experimental period at the FO_3X. AOT40 was calculated using hourly O_3 concentration data during the daytime (with solar radiation exceeding 50 W m^{-2}; CLRTAP, 2017). It is given by:

$$AOT40 = \sum max([O_3] - 40, 0)\cdot dt \tag{1}$$

where $[O_3]$ is the hourly O_3 concentration (ppb) and dt denotes the time step (=1 h). On the other hand, POD_Y was calculated following the standard methodology recommended by CLRTAP (2017):

$$POD_Y = \sum max(F_{st} - Y, 0)\cdot dt \tag{2}$$

where F_{st} denotes hourly stomatal O_3 flux (nmol m^{-2} s^{-1}). F_{st} can be calculated according to a resistance analogy as:

$$F_{st} = [O_3]\cdot g_s \cdot \frac{r_c}{r_b + r_c} \tag{3}$$

where g_s represents stomatal conductance for O_3 (mmol O_3 m^{-2} PLA [Projected Leaf Area] s^{-1}). r_b denotes leaf boundary layer resistance, which is determined based on wind speed and leaf dimensions (4 cm), while r_c is leaf surface resistance expressed as $1/(g_s + g_{ext})$ (s m^{-1}), where g_{ext} denotes the cuticular conductance (0.0004 s m^{-1}, CLRTAP, 2017). For further details for r_b and r_c, refer to CLRTAP (2017).

2.4. Stomatal conductance model and parametrization

A simplified equation of the multiplicative g_s model was utilized due to the well-watered conditions (and thus no effects of soil water deficit on g_s) in which all plants were grown at the FO_3X (Hoshika et al., 2020; Manzini et al., 2025). This simplified model is expressed as:

$$g_s = g_{max}\cdot f_{light}\cdot max\left\{f_{min}, \left(f_{temp}\cdot f_{VPD}\cdot f_{O3}\right)\right\} \tag{4}$$

where g_{max} is the maximum stomatal conductance (mmol O_3 m^{-2} PLA s^{-1}), f_{min} is the minimum conductance, which is expressed as 0 to 1, f_{light}, f_{temp}, $f_{VPD,}$ and f_{O3} denote the response functions of g_s to PPFD, T, and vapor pressure deficit (VPD), respectively.

The equation of f_{light} is denoted as:

$$f_{light} = 1 - \exp(-a\cdot PPFD) \tag{5}$$

where a is a coefficient that defines the shape of the exponential stomatal light response.

The f_{temp} is given by:

$$f_{temp} = \left(\frac{T - T_{min}}{T_{opt} - T_{min}}\right)\left\{\left(\frac{T_{max} - T}{T_{max} - T_{opt}}\right)^{\left(\frac{T_{max}-T_{opt}}{T_{opt}-T_{min}}\right)}\right\} \tag{6}$$

where T_{opt} denotes the optimal temperature for stomatal opening and T_{min} and T_{max} are the minimum and maximum temperature (°C) for g_s, respectively (T_{min} and T_{max} were set to 4 and 45 °C, respectively; Matta and Maestri, 1997; Silva et al., 2004; Yamane et al., 2022).

The f_{VPD} is given by:

$$f_{VPD} = \frac{(1 - f_{min})\cdot(VPD_{min} - VPD)}{VPD_{min} - VPD_{max}} + f_{min} \tag{7}$$

where VPD_{min} and VPD_{max} indicate the VPD threshold for achieving minimum and maximum g_s, respectively.

The f_{O3} is given by:

$$f_{O3} = 1 - q \times [O_3] \tag{8}$$

where q denotes the reduction rate of g_s with O_3 concentration.

To parameterize the g_s model, g_s for coffee cultivars was measured by using a portable flow-through differential porometer (LI600, Li-Cor, Lincoln, USA). Measurements were carried out across the experimental period (1–3 times per month, total of 6 days for Geisha cultivar and 5 days for IAC62 and IAC99 cultivars) on sun-exposed leaves under various environmental conditions. Pooled data (621 data points in Geisha cultivar, 282 data points in IAC62, and 218 data points in IAC99) were used to parametrize the multiplicative g_s model according to the boundary-line technique (Braun et al., 2010; Hoshika et al., 2020). In addition to these training data, additional datasets for g_s were obtained (two days measured for Geisha [12th July and August 10, 2022, a total of 137 data points] and two days measured for IAC62 and IAC99 [12th and July 13, 2023, total of 37 and 41 data points for IAC62 and IAC99, respectively]) for the validation of the stomatal models.

For the parametrization, data of g_s were separated into categories with incremental steps for each environmental variable: 200 μmol m^{-2} s^{-1} for PPFD (but 50 μmol m^{-2} s^{-1} steps were applied when PPFD <200 μmol m^{-2} s^{-1}), 2 °C for T, 0.4 kPa for VPD, and 20 ppb for O_3. Each model function was then fitted based on the 95th percentile values for each category of environmental factors. The g_{max} value was obtained as the 95th percentile value recorded during the experiment, while f_{min} was set to the ratio of the 5th percentile value against g_{max}.

2.5. Dose-response (DR) relationship and derivation of critical levels (CLs)

The DR relationships for LB were established based on exposure and flux indexes (AOT40 and POD_Y). We employed the extrapolation method proposed by Paoletti et al. (2017) to calculate a relative LB reduction. This method assumes that the biomass linearly declines relative to a pre-industrial O_3 level (24 h means O_3 concentration, M24 = 10 ppb). The intercept was set as 1, and the linear function between O_3 indexes and LB, showing the highest coefficient of determination (R^2), was selected to calculate CLs. No higher thresholds were examined after Y = 3 nmol m^{-2} s^{-1}, because POD_3 values in the three cultivars were lower than 0.01, thus negligible.

Using the best Y threshold, CLs corresponding to a 4 % (CLRTAP, 2017) and 10 % biomass reduction were calculated using either linear regressions or the four-parameter Lorentz nonlinear regression model, which Hoshika et al. (2024a,b) suggested as one of the best nonlinear functions for the O_3 risk assessment. The threshold of 10 % was included to ensure comparability between the cultivars. The models were compared based on the Akaike Information Criterion (AIC) values. To gain a comprehensive understanding of the data and provide comparable CLs with the ICP-Vegetation Manual (CLRTAP, 2017), CLs were also calculated using AOT40 and POD_1.

2.6. Statistical analysis

The total LB of each *C. arabica* cultivar was averaged per plot ($n = 3$), and normal distribution (Kolmogorov-Smirnov test), as well as homogeneity of variance (Levene's test), were checked. Differences between O_3 treatments (i.e., AA, 1.5 ×, 2.0 ×), cultivars (i.e., Geisha, IAC62, IAC99), and their interaction were tested by two-way analysis of variance (ANOVA). Linear and nonlinear regression analyses (four-parameter Lorentz nonlinear regression model) were performed for the DR relationships between LB and O_3 indices.

Although the Geisha cultivar was exposed to three O_3 levels (AA, 1.5 × AA, 2.0 × AA) and the IAC62 and IAC99 cultivars to only two levels (AA and 2.0 × AA), the statistical comparability of dose–response (DR) relationships across cultivars was ensured by two methodological choices. First, we calculated biomass response in relative terms, normalizing leaf biomass production to values at the beginning of the experiment, which were available for each cultivar. This allowed us to assess biomass accumulation during the O_3 exposure period and not absolute values, reducing the influence of initial differences. Second, we adopted a flux-based approach ($POD_{1.5}$) that integrates stomatal O_3 uptake over time. This physiological index reflects the actual dose of O_3 entering the leaf tissue, regardless of the exposure levels, and accounts for cultivar-specific differences in g_s and environmental conditions. The use of a continuous variable such as $POD_{1.5}$, instead of discrete treatment classes, enables linear regression modeling of DR responses across cultivars on a common scale. This approach is aligned with CLRTAP recommendations and has been successfully applied in other multi-cultivar studies (e.g., Hoshika et al., 2024a,b). Therefore, despite the different experimental designs, our analysis framework allowed a robust comparison of O_3 sensitivity among coffee cultivars.

Statistical significance was considered at $p < 0.05$. All the statistical analyses were conducted using Origin Lab software®.

3. Results

3.1. Total leaf biomass (LB) and O_3 visible foliar injury (O_3_VFI)

Ozone significantly reduced total LB in *C. arabica* cultivar ($p < 0.01$, Table 1). In detail, the Geisha and IAC62 cultivars showed a significant decrease between AA and 2.0 ×, while differences in total LB were not found in IAC99. In addition, we observed a statistically significant difference ($p < 0.001$) of this parameter among the cultivar considered (Geisha > IAC99 > IAC62) and a significant interaction ($p < 0.05$) between O_3 and the cultivar.

Regarding the presence of O_3_VFI on fully developed leaves within the O_3_FACE facility, plants from the control treatment exhibited no specific O_3_VFI, retaining a uniformly green appearance and displaying no signs of photoxidative stress (Fig. 2A). In contrast, plants subjected to O_3 treatment developed small, interveinal chlorotic injuries uniformly distributed across the leaf surface, indicating the onset of oxidative damage. For leaves of Geisha, developed before exposure, the interaction between O_3 effect and photooxidative stress was clearly evident. A total of 16.1 % of AA leaves exhibited injury (Fig. 2C) possibly due to photooxidation alone, of which 7.7 % were related to reddening (47 % of the total injury), 4.5 % browning (4.5 % of the total injury) and 4.0 % to chlorosis (25 % of the total injury). In contrast, in 2.0 × plants 32.8 % of the samples presented VFI (Fig. 2C), of which 20.3 % were related to reddening (62 % of the total injury), 5.0 % browning (15 % of the total injury) and 7.4 % to chlorosis (23 % of the total injury).

Table 1
Total leaf biomass (LB - average values ± standard error) of *C. arabica* cultivar (Geisha, IAC62, and IAC99), exposed to O_3 treatments (AA, 1.5 ×, and 2.0 ×). Different letters indicate significant differences among O_3 treatments for each cultivar following two-way ANOVA and Tukey test (*$p < 0.05$, **$p < 0.01$, ***$p < 0.001$, $n = 3$).

Cultivar	O_3 treatment	Total LB (g)
Geisha	AA	7.79 ± 0.45 a
	1.5 ×	6.71 ± 0.51 ab
	2.0 ×	5.70 ± 0.18 b
IAC62	AA	1.42 ± 0.22 α
	2.0 ×	0.71 ± 0.10 β
IAC99	AA	3.41 ± 0.41 A
	2.0 ×	3.10 ± 0.38 A
Two-way ANOVA		
	O_3	**
	Cultivar	***
	O_3 × Cultivar	*

3.2. Parameters of g_s model for coffee plants

Overall, no significant differences in g_s among the cultivars were observed. Mean values were nearly identical across cultivars (mean ± standard deviation: 0.028 ± 0.01 μmol m^{-2} s^{-1} for IAC62 and IAC99, and 0.027 ± 0.01 μmol m^{-2} s^{-1} for Geisha) and the one-way ANOVA confirmed the absence of statistically significant differences among cultivars ($p = 0.89$).

Also parameterized g_s values were similar among the cultivars. The parameters of g_s model are shown in Table 2 and Appendix Figure S1. The g_{max} values were 51, 59, and 45 mmol O_3 m^{-2} PLA s^{-1} in Geisha, IAC62, and IAC99 cultivars, respectively. The f_{min} was similar among the three cultivars (approx. 0.01). The limiting functions of g_s characterized the stomatal response to environmental factors for coffee cultivars. The f_{light} followed a sharp increase of g_s in the low light range (<200 μmol m^{-2} s^{-1}) regardless of the different cultivars. The f_{temp} indicated an optimal temperature for the stomatal opening around 26–28 °C in three cultivars. According to the f_{VPD}, IAC99 cultivars had a slightly sharper decrease in g_s when increasing VPD compared to Geisha and IAC62 cultivars. Stomatal conductance response to O_3 was cultivar-specific, where the slope parameter (q) was relatively high in IAC62, suggesting that g_s sharply decreases with increasing [O_3] in this cultivar. On the other hand, in IAC99, the O_3-induced decrease in c was rather moderate, as confirmed by a lower q value (0.0029). The model estimates of g_s agreed with the measured g_s values in three cultivars, although the model tended to slightly overestimate the low g_s range (Fig. 3).

The sensitivity analysis assessed uncertainty in the g_s model parameters affected by POD_1 estimates for three coffee cultivars. Each Jarvis-type model parameter (f_{light}, f_{temp}, f_{VPD}, f_{O3}) was perturbed by ±10 %

Table 2
Summary of g_s model parameters for three coffee cultivars (Geisha, IAC62, IAC99) grown under the Free-air O_3 eXposure (FO_3X) experiments. g_{max} denotes the maximum stomatal conductance; f_{min} is a fraction as a ratio of minimum conductance to g_{max}; f_{light}, f_{temp}, $f_{VPD,}$ and f_{O3} are the stomatal response functions against environmental factors (photosynthetic photon flux density, PPFD; temperature, T; vapor pressure deficit, VPD; and O_3 concentration, O_3); a is the coefficient determining a curvature of f_{light}; T_{opt} denotes optimal temperature for stomatal opening; T_{min} and T_{max} denote minimum and maximum temperature causing a limitation of gas exchange, which were set to 4 and 45 °C, respectively, according to the previous studies (DaMatta and Ramalho, 2006; Silva et al., 2004; Yamane et al., 2022); VPD_{min} and VPD_{max} denote the threshold of VPD where g_s reached its minimum and maximum, respectively; q denotes the reduction rate of g_s with O_3 concentration.

Parameter			Geisha	IAC62	IAC99
g_{max}	(mmol O_3 m^{-2}PLA s^{-1})		51	59	45
f_{min}		(fraction)	0.08	0.09	0.11
f_{light}	a	(constant)	0.0147	0.0146	0.0125
f_{temp}	T_{opt}	(°C)	28	27	26
	T_{min}	(°C)	4	4	4
	T_{max}	(°C)	45	45	45
f_{VPD}	VPD_{max}	(kPa)	1.9	2.0	1.5
	VPD_{min}	(kPa)	7.6	7.4	6.1
f_{O3}	q	(kPa)	0.0036	0.0042	0.0028

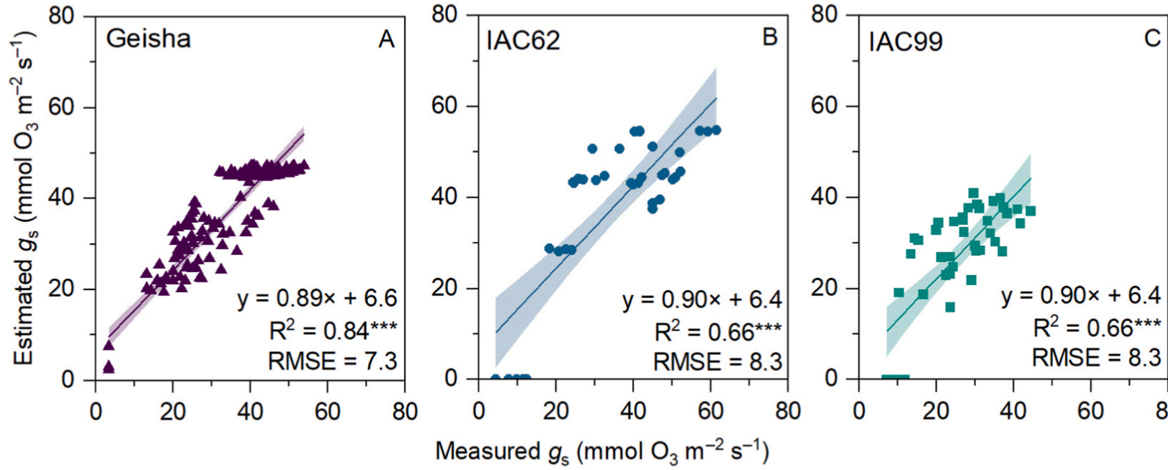

Fig. 3. Comparison between measured and estimated stomatal conductance (g_s) for three coffee cultivars (Geisha, IAC62, IAC99) grown under the Free-air O_3 eXposure (FO_3X) experiments. Linear regression analysis: ***$p < 0.001$; RMSE = Root-Mean-Square Error.

and ±20 %, and the changes in POD_1, R^2, and RMSE recorded (Table S3). POD_1 values mostly stayed within ±10 % of baseline across cultivars and parameters, indicating that the model outputs are generally robust to moderate parameter uncertainty.

These results suggest that the cultivar factor did not significantly influence the observed variation in g_s. Therefore, consistent with previous findings in other tropical tree species (Moura et al., 2021), the dose–response (DR) relationships and critical levels (CLs) were calculated considering the Coffea species as a whole, to ensure the broader applicability of the results.

3.3. Dose-response (DR) relationships for coffee plants and critical levels (CLs)

Among the DR relationships evaluated, $POD_{1.5}$ exhibits the highest coefficient of determination ($R^2 = 0.99$, Table S2), and was chosen as the best Y threshold.

Linear and nonlinear regression models were applied to estimate the O_3 critical levels (CLs) associated with biomass (LB) reduction in *C. arabica*. The linear model was selected based on its superior statistical performance (Fig. 4A, Fig. S3A), showing a strong and significant relationship between O_3 concentration and relative biomass increment ($R^2 = 0.99$, $p < 0.0001$, AIC = 28.91) with low residual error (RSS = 0.041). In contrast, the Lorentzian model showed a poor fit to the data ($R^2 = 0.34$, $p > 0.05$, AIC = 42.77), higher residual error (RSS = 0.143), and thus, large uncertainty in parameter estimates (Fig. S2, Fig. S3B).

Considering 4 % biomass reduction, the calculated CL was 0.29 mmol m^{-2} $POD_{1.5}$. The POD_1 estimated a CL of 0.53 mmol m^{-2} (Fig. 4B), and the AOT40 estimated a CL of 3.85 ppm h (Fig. 4C). For 10 % biomass reduction, the calculated CL was 0.73 mmol m^{-2} $POD_{1.5}$. The POD_1 linear regression estimated a CL of 1.34 mmol m^{-2} (Fig. 4B), and the AOT40 estimated a CL of 9.96 ppm h (Fig. 4C).

4. Discussion

4.1. Biomass responses to O_3 exposure

Ozone exposure significantly reduced LB in two of the three *C. arabica* cultivars, with Geisha and IAC62 being more susceptible to O_3 than IAC99. This cultivar-specific variation in sensitivity aligns with findings in other species, such as the tropical species *Moringa oleifera*, where even different ecotypes exhibited varying degrees of biomass loss under O_3 exposure (Moura et al., 2024). The O_3 resistance mechanisms of different cultivars may be associated with differences in the stomatal regulation capacity, specific capacity to allocate primary and secondary metabolites, and detoxification capacity linked with antioxidative mechanisms.

The present study reports the presence of O_3_VFI in *C. arabica* cultivars for the first time, with a clear synergy with photooxidative stress due to higher light intensity, thus increasing the deleterious effect of O_3.

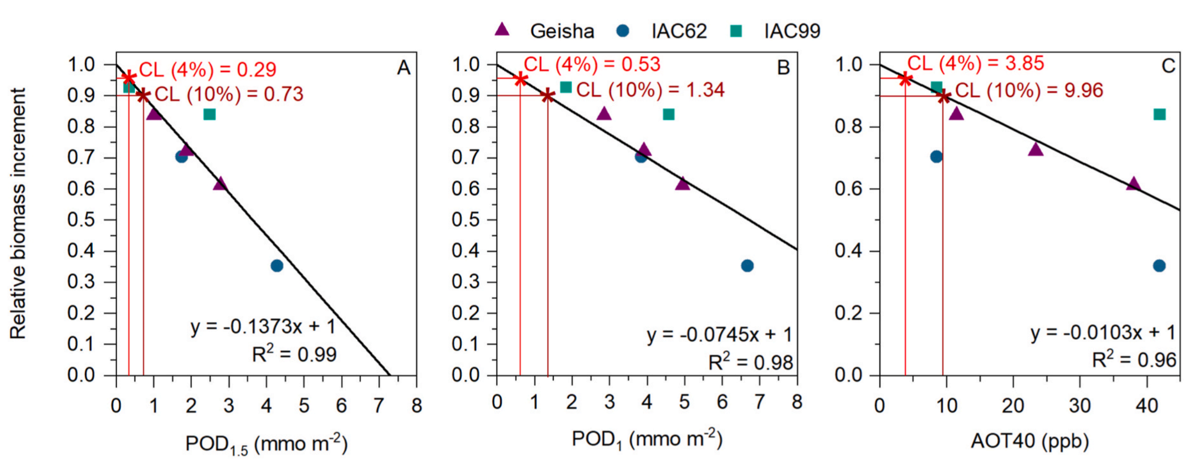

Fig. 4. Relative biomass increments in *C. arabica* cultivars as a function of the Phytotoxic O_3 Dose ($POD_{1.5}$ and POD_1) and the exposure-bases index (AOT40). Linear regression (solid line). Different symbols represent distinct cultivars. Data is represented in leaf biomass dry weight.

Genes that control cell death respond differently to O_3 and high light, with high light increasing O_3-driven cell death in leaves (Xu et al., 2022), which resembles a hypersensitive response-like mechanism, which involves programmed cell death as part of the plant defense strategy as widely documented in response to oxidative stress across species (Vollenweider et al., 2003). The progression of chlorotic spots into necrotic lesions suggests that the detoxification mechanisms were overwhelmed, as demonstrated in other sensitive species (Moura et al., 2011).

4.2. Stomatal regulation due to O_3 exposure

The cultivar-specific biomass loss observed in this study can be primarily attributed to differences in g_{max}, across the cultivars. As expected, the cultivars with higher g_{max}, such as IAC62 and Geisha, experienced more pronounced reductions in LB compared to IAC99, which had a lower g_{max}. This trend is consistent with findings in other plant species, such as hybrid poplar clones, where higher g_{max} was linked to increased O_3 uptake and more severe oxidative stress, ultimately leading to greater biomass loss (Hoshika et al., 2018, 2024a,b).

The variation in g_{max} among the present cultivars reflected inherent differences in gas exchange capacities. A relatively low g_s in the IAC99 cultivar was similarly reported, relating to its high tolerance against water stress (Lisboa et al., 2021). While the f_{min} values were similar across cultivars, indicating a stable baseline for gas exchange, the other limiting functions of g_s, including responses to light (f_{light}), temperature (f_{temp}), and vapor pressure deficit (f_{VPD}), characterized stomatal response patterns for coffee plants. For instance, the optimal temperature for stomatal opening was consistent across cultivars (26–28 °C), which is within the range observed in other studies on tropical crops (Moura et al., 2018b). Interestingly, IAC99 showed a sharper decline in g_s with increasing VPD, indicating a higher sensitivity to atmospheric dryness than Geisha and IAC62. This high stomatal sensitivity to VPD likely limits IAC99 gas exchange under stressful conditions in the afternoon when VPD and O_3 concentrations were elevated, protecting it from excessive O_3 uptake and oxidative stress. A moderate stomatal closure response to elevated O_3 concentration was observed in IAC99, which was reflected in its lower q value (0.0029), indicating a high tolerance capacity of this cultivar under elevated O_3. In contrast, IAC62 exhibited a sharp decline in g_s with increasing O_3 concentration, as indicated by its higher slope parameter ($q = 0.0042$). This suggests that IAC62 is more sensitive to O_3 regarding stomatal regulation, which likely contributes to a limited CO_2 uptake via stomata, thus resulting in a greater reduction in LB under O_3 stress. Previous studies have shown similar patterns in other tropical crop species, such as sugarcane, where cultivars with higher O_3 sensitivity exhibited more significant reductions in biomass due to impaired stomatal function (Moura et al., 2018a, 2018b).

4.3. Ozone critical levels (CLs) for coffee biomass production

For the species *C. arabica*, the Phytotoxic O_3 Dose (POD_Y) consistently showed a better performance to express the DR relationship between O_3 levels and LB of coffee cultivars than the exposure-bases index (AOT40). The $POD_{1.5}$ was chosen as the best threshold for the species. However, a threshold of $Y = 6$ nmol m^{-2} s^{-1} has been proposed for crops in the ICP Vegetation Manual (CLRTAP, 2017); for coffee cultivars, this threshold cannot be applied, because the accumulated POD_3 was lower than 0.01 and neglectable. In fact, the threshold of 6 nmol m^{-2} s^{-1} (POD_6) remains under debate for tree crops and perennial fruit plants, as their g_s is typically lower than that of annual crops (Moura et al., 2023).

The linear regression was demonstrated to be appropriate for assessing the DR relationship between O_3 levels and LB of coffee cultivars. However, the CL calculated using linear regression was around 83 % lower than when compared to the nonlinear regression approach. The use of linear models alone may oversimplify the DR relationship, particularly at low sub-toxic doses, which often stimulate organisms and prime them for tolerance against more severe stress (Volkova et al., 2022; Manzini et al., 2025). This hormetic zone tends to shift towards higher doses as plant tolerance to O_3 increases (Agathokleous et al., 2020). In fact, in recent studies, the DR relationships were successfully drawn by nonlinear functions, especially for moderately or resistant species (Hoshika et al., 2024a,b), which was not the case for coffee cultivars, which were demonstrated to be highly sensitive to the O_3 effects.

Still, according to the ICP Vegetation Manual, POD_1 is commonly used to estimate O_3-induced biomass loss in sensitive tree species (CLRTAP, 2017) and thus was applied in the present study. In this case, the POD_1 CL calculated for coffee cultivars of 5.37 mmol m^{-2} reveals its high sensitivity to the O_3 effect once the POD_1 CL recommended in the ICP-Vegetation Manual range from 5.2 mmol m^{-2} for beech and birch (very sensitive species) up to 47.3 mmol m^{-2} for Mediterranean evergreen species (tolerant species).

4.4. Study limitations

Filling the knowledge gap on O_3 effects in tropical plant species remains a significant challenge, as this field is currently addressed by only a limited number of research groups. Studies such as the present one, conducted in facilities located outside tropical regions, can provide important insights but are inherently limited to indicative responses. One key limitation of our study is that the experiment was carried out over two distinct years, due to logistical constraints in plant propagation and transportation. To mitigate this, we normalized physiological responses and adopted a flux-based approach to account for plant-specific O_3 uptake, thereby enhancing comparability. Nonetheless, subtle year-specific environmental interactions cannot be entirely excluded. A second limitation concerns the replication structure of conducting experiments in a FACE where the number of replicated plots per treatment is limited, reducing statistical power and limiting the detection of finer-scale treatment effects. Finally, only a limited number of cultivars were included in this study. Although g_s did not differ significantly among them, the observed responses may not represent the full diversity of *Coffea* cultivars. Expanding the range of cultivars and including multiple geographic locations would increase the robustness and applicability of the critical thresholds derived from this research. Future studies could specifically address this gap by testing a broader set of genetic backgrounds and environmental conditions, thereby strengthening the generalization of the findings to diverse coffee-growing regions.

5. Conclusions

This study highlights the significant impact of O_3 exposure on *C. arabica* cultivars. Geisha and IAC62 were more sensitive cultivars, experiencing greater reductions in LB, while IAC99 was more resistant. The occurrence of O_3-induced O_3_VFI, reported here for the first time for Geisha cultivar, suggests that detoxification mechanisms were overwhelmed under high O_3 levels. We encourage researchers and coffee production farms to search for similar O_3_VFI in field conditions to corroborate these findings; however, additional microscopic or anatomical validations would be needed to confirm the source of the symptom.

Stomatal regulation played a key role in determining O_3 sensitivity, with cultivars exhibiting higher stomatal conductance (g_{max}) showing more severe biomass losses. IAC99, with lower g_{max} and higher sensitivity to VPD, was more protected from excessive O_3 uptake.

The CLs of O_3 exposure, defined by the flux-based index $POD_{1.5}$ and POD_1, provide valuable insights for managing O_3 risks in coffee cultivation. Future research should focus on understanding O_3 sensitivity mechanisms and exploring effective strategies to enhance *C. arabica* resilience in regions facing rising O_3 pollution.

CRediT authorship contribution statement

Barbara Baesso Moura: Writing – original draft, Visualization, Formal analysis, Data curation, Conceptualization. **Marisa Domingos:** Project administration, Funding acquisition. **Emerson Alves da Silva:** Methodology, Conceptualization. **Jacopo Manzini:** Investigation, Data curation. **Elena Marra:** Writing – original draft, Methodology. **Leonardo Lazzara:** Methodology, Investigation. **Rodrigo Fazani Esteves Sanches:** Methodology, Investigation. **Elena Paoletti:** Supervision, Conceptualization. **Yasutomo Hoshika:** Project administration, Funding acquisition, Data curation.

Declaration of generative AI in scientific writing

During the preparation of this work, the authors used OpenAI/ChatGPT and Grammarly to improve the manuscript's readability and language. After using this tool/service, the authors reviewed and edited the content as needed and takes full responsibility for the content of the published article.

Declaration of competing interest

The authors declare that they have no known competing financial interests or personal relationships that could have appeared to influence the work reported in this paper.

The author is an Editorial Board Member/Editor-in-Chief/Associate Editor/Guest Editor for this journal and was not involved in the editorial review or the decision to publish this article.

Acknowledgements

We thank Alessandro Materassi and Moreno Lazzara for technical support. We thank for financial support to Fondazione Cassa di Risparmio di Firenze (2013/7956); Bilateral Agreement of CNR and FAPESP 2022–2023 (B85F22000090005) 'Environmental impacts of ozone and climatic changes on major Brazilian crops (sugarcane and coffee cultivars)'; PNRR for Mission 4 (Component 2, Notice 3264/2021, IR0000032) - ITINERIS - CUP B53C22002150006; and Project funded under the National Recovery and Resilience Plan (NRRP), Mission 4 Component 2 Investment 1.4 - Call for tender No. 3138 of December 16, 2021, rectified by Decree n.3175 of December 18, 2021 of Italian Ministry of University and Research funded by the European Union – NextGenerationEU, Award Number: Project code CN_00000033, Concession Decree No. 1034 of June 17, 2022 adopted by the Italian Ministry of University and Research, CUP, H43C22000530001 Project title "National Biodiversity Future Center - NBFC" (Spoke 3 and 5).

Appendix A. Supplementary data

Supplementary data to this article can be found online at https://doi.org/10.1016/j.apr.2025.102768.

Data availability

All raw datasets generated or analyzed in this study, including raw AOT40, PODy, biomass, and g_s measurements, can be provided by the corresponding author upon reasonable request.

References

Abreu Júnior, C.A.M.D., Martins, G.D., Xavier, L.C.M., Vieira, B.S., Gallis, R.B.D.A., Fraga Junior, E.F., Martins, R.S., Paes, A.P.B., Mendonça, R.C.P., Lima, J.V.D.N., 2022. Estimating coffee plant yield based on multispectral images and machine learning models. Agronomy 12 (12), 3195.

Agathokleous, E., Feng, Z., Oksanen, E., Sicard, P., Wang, Q., Saitanis, C.J., Araminiene, V., Blande, J.D., Hayes, F., Calatayud, V., Domingos, M., Veresoglou, S. D., Peñuelas, J., Wardle, D.A., Marco, A.D., Li, Z., Harmens, H., Yuan, X., Vitale, M., Paoletti, E., 2020. Ozone affects plant, insect, and soil microbial communities: a threat to terrestrial ecosystems and biodiversity. Sci. Adv. 6 (33), eabc1176.

Agrawal, S.B., Agrawal, M., Singh, A., 2021. Tropospheric Ozone: a Hazard for Vegetation and Human Health. Cambridge Scholars Publishing.

Bernardes, T., Moreira, M.A., Adami, M., Giarolla, A., Rudorff, B.F.T., 2012. Monitoring biennial bearing effect on coffee yield using MODIS remote sensing imagery. Remote Sens. 4 (9), 2492–2509.

Braun, S., Schindler, C., Leuzinger, S., 2010. Use of sap flow measurements to validate stomatal functions for mature beech (*Fagus sylvatica*) in view of ozone uptake calculations. Environ. Pollut. 158 (9), 2954–2963.

Cheesman, A.W., Brown, F., Farha, M.N., Rosan, T.M., Folberth, G.A., Hayes, F., Moura, B.B., Paoletti, E., Hoshika, Y., Osborne, C.P., Cernusak, L.A., Ribeiro, R.V., Sitch, S., 2023. Impacts of ground-level ozone on sugarcane production. Sci. Total Environ. 904, 166817.

CLRTAP, 2017. Mapping critical levels for vegetation, chapter III of manual on methodologies and criteria for modelling and mapping critical loads and levels and air pollution effects, risks and trends. UNECE convention on Long-range transboundary air pollution. www.icpmapping.org. (Accessed 1 May 2024).

CONAB, 2024. Acompanhamento da Safra Brasileira 2023/2024. Companhia Nacional de Abastecimento (CONAB) 11 (2318 6852), 110. https://www.conab.gov.br/info-agro/safras/.

DaMatta, F.M., Ramalho, J.D.C., 2006. Impacts of drought and temperature stress on coffee physiology and production: a review. Braz. J. Plant Physiol. 18, 55–81.

Feng, Z., Xu, Y., Kobayashi, K., Dai, L., Zhang, T., Agathokleous, E., Calatayud, V., Paoletti, E., Mukherjee, A., Agrawal, M., Park, R.J., Oak, Y.j., Yue, X., 2022. Ozone pollution threatens the production of major staple crops in East Asia. Nat. Food 3 (1), 47–56.

Hertel, T.W., 2016. Food security under climate change. Nat. Clim. Change 6 (1), 10–13.

Hoshika, Y., Moura, B.B., Paoletti, E., 2018. Ozone risk assessment in three oak species as affected by soil water availability. Environ. Sci. Pollut. Control Ser. 25 (9), 8125–8136. https://doi.org/10.1007/s11356-017-9786-7. Epub 2017 Jul 27. PMID: 28748441.

Hoshika, Y., Paoletti, E., Agathokleous, E., Sugai, T., Koike, T., 2020. Developing ozone risk assessment for larch species. Frontiers in Forests and Global Change 3, 45.

Hoshika, Y., Agathokleous, E., Moura, B.B., Paoletti, E., 2024a. Ozone risk assessment with free-air controlled exposure (FACE) experiments: a critical revisit. Environ. Res. 255, 119215. https://doi.org/10.1016/j.envres.2024.119215. ISSN 0013-9351.

Hoshika, Y., Pollastrini, M., Marzuoli, R., Gerosa, G., Marra, E., Moura, B.B., Agathokleous, E., Calatayud, V., Feng, Z., Sicard, P., Paoletti, E., 2024b. Unraveling the difference of sensitivity to ozone between non-hybrid native poplar and hybrid poplar clones: a flux-based dose-response analysis. Environ. Pollut. 1 (358), 124524. https://doi.org/10.1016/j.envpol.2024.124524. Epub 2024 Jul 8. PMID: 38986760.

Kobayashi, K., 2022. Effects of ozone on agricultural crops. In: Handbook of Air Quality and Climate Change. Springer Nature Singapore, Singapore, pp. 1–44.

Lisboa, L.A.M., Cunha, M.L.O., Nakayama, F.T., de Figueiredo, P.A.M., da Silva Viana, R., Ramos, S.B., Ferrari, S., 2021. Morphophysiological characteristics of Arabic coffee. Nativa 9 (1), 36–43.

Manzini, J., Hoshika, Y., Danti, R., Moura, B.B., Paoletti, E., Della Rocca, G., 2025. Ozone risk assessment of common cypress (*Cupressus sempervirens* L.) clones and effects of *Seiridium cardinale* infection. J. Environ. Sci. 151, 441–453.

Matta, F.M., Maestri, M., 1997. Decline of vegetative growth in *Coffea arabica* L. in relation to leaf temperature, water potential and stomatal conductance. Field Crops Res. 54 (1), 65–72.

Medrano, Juan F., Cantu, D., Minio, A., Dreischer, C., Gibbons, T., Chin, J., Chen, S., Van Deynze, A., Hulse-Kemp, A.M., 2025. De novo whole-genome assembly and annotation of *Coffea arabica* var. Geisha, a high-quality coffee variety from the primary origin of coffee. G3: Genes, Genomes, Genetics 15 (1) jkae262.

Menezes-Silva, P.E., Sanglard, L.M., Ávila, R.T., Morais, L.E., Martins, S.C., Nobres, P., Patreze, C.M., Ferreira, M.A., Araújo, W.L., Fernie, A.R., DaMatta, F.M., 2017. Photosynthetic and metabolic acclimation to repeated drought events play key roles in drought tolerance in coffee. J. Exp. Bot. 68 (15), 4309–4322.

Mills, G., Pleijel, H., Malley, C.S., Sinha, B., Cooper, O.R., Schultz, M.G., Neufeld, H.S., Simpson, D., Sharps, K., Feng, Z., Gerosa, G., Harmens, H., Kobayashi, K., Saxena, P., Paoletti, E., Sinha, V., Xu, X., 2018. Tropospheric ozone assessment report: Present-day tropospheric ozone distribution and trends relevant to vegetation. Elementa Science Anthropocene 6, 47.

Miyazaki, K., Eskes, H., Sudo, K., Boersma, K.F., Bowman, K., Kanaya, Y., 2017. Decadal changes in global surface NOx emissions from multi-constituent satellite data assimilation. Atmos. Chem. Phys. 17 (2), 807–837.

Moura, B.B., Souza, S.R.D., Alves, E.S., 2011. Structural responses of *Ipomoea nil* (L.) Roth'Scarlet O'Hara' (Convolvulaceae) exposed to ozone. Acta Bot. Bras. 25, 122–129.

Moura, B.B., Alves, E.S., de Souza, S.R., Domingos, M., Vollenweider, P., 2014. Ozone phytotoxic potential with regard to fragments of the Atlantic Semi-deciduous forest downwind of Sao Paulo, Brazil. Environ. Pollut. 192, 65–73.

Moura, B.B., Hoshika, Y., Ribeiro, R.V., Paoletti, E., 2018a. Exposure- and flux-based assessment of ozone risk to sugarcane plants. Atmos. Environ. 176, 252–260. https://doi.org/10.1016/j.atmosenv.2017.12.039. ISSN 1352-2310.

Moura, B.B., Hoshika, Y., Silveira, N.M., Marcos, F.C., Machado, E.C., Paoletti, E., Ribeiro, R.V., 2018b. Physiological and biochemical responses of two sugarcane genotypes growing under free-air ozone exposure. Environ. Exp. Bot. 153, 72–79.

Moura, B.B., Brunetti, C., Engela, M.R. G. da S., Hoshika, Y., Paoletti, E., Ferrini, F., 2021. Experimental assessment of ozone risk on ecotypes of the tropical tree *Moringa oleifera*. Environ. Res. 201. https://doi.org/10.1016/j.envres.2021.111475.

Moura, B.B., Manzini, J., Paoletti, E., Hoshika, Y., 2023. A three-year free-air experimental assessment of ozone risk on the perennial *Vitis vinifera* crop species. Environ. Pollut. 338, 122626.
Moura, B.B., Hoshika, Y., Brunetti, C., dos Santos Nascimento, L.B., Marra, E., Paoletti, E., Ferrini, F., 2024. Stress physiology of *Moringa oleifera* under tropospheric ozone enrichment: an ecotype-specific investigation into growth, nonstructural carbohydrates, and polyphenols. Plant J. https://doi.org/10.1111/tpj.17107.
Paoletti, E., Materassi, A., Fasano, G., Hoshika, Y., Carriero, G., Silaghi, D., Badea, O., 2017. A new-generation 3D ozone FACE (free air controlled exposure). Sci. Total Environ. 575, 1407–1414.
Rodrigues, W.P., Silva, J.R., Ferreira, L.S., Machado Filho, J.A., Figueiredo, F.A., Ferraz, T.M., Bernado, W.P., Bezerra, L.B.S., de Abreu, D.P., Cespom, C., Ramalho, J. C., Campostrini, E., 2018. Stomatal and photochemical limitations of photosynthesis in coffee (Coffea spp.) plants subjected to elevated temperatures. Crop Pasture Sci. 69 (3), 317–325.
Sanches, R.F.E., da Cruz Centeno, D., Braga, M.R., da Silva, E.A., 2020. Impact of high atmospheric CO_2 concentrations on the seasonality of water-related processes, gas exchange, and carbohydrate metabolism in coffee trees under field conditions. Clim. Change 162, 1231–1248.
Sicard, P., 2021. Ground-level ozone over time: an observation-based global overview. Current Opinion in Environmental Science & Health 19, 100226.
Silva, E.A., DaMatta, F.M., Ducatti, C., Regazzi, A.J., Barros, R.S., 2004. Seasonal changes in vegetative growth and photosynthesis of Arabica coffee trees. Field Crops Res. 89 (2–3), 349–357.
Singh, A.A., Fatima, A., Mishra, A.K., Chaudhary, N., Mukherjee, A., Agrawal, M., Agrawal, S.B., 2018. Assessment of ozone toxicity among 14 Indian wheat cultivars under field conditions: growth and productivity. Environ. Monit. Assess. 190 (4), 190.
Vazquez Santiago, J., Hata, H., Martinez-Noriega, E.J., et al., 2024. Ozone trends and their sensitivity in global megacities under the warming climate. Nat. Commun. 15, 10236. https://doi.org/10.1038/s41467-024-54490-w.
Volkova, P.Y., Bondarenko, E.V., Kazakova, E.A., 2022. Radiation hormesis in plants. Current Opinion in Toxicology 30, 100334.
Vollenweider, P., Ottiger, M., Günthardt-Goerg, M.S., 2003. Validation of leaf ozone symptoms in natural vegetation using microscopical methods. Environ. Pollut. 124 (1), 101–118.
Xu, E., Tikkanen, M., Seyednasrollah, F., Kangasjärvi, S., Brosché, M., 2022. Simultaneous ozone and high light treatments reveal an important role for the chloroplast in Co-ordination of defense signaling. Front. Plant Sci. 13, 883002. https://doi.org/10.3389/fpls.2022.883002.
Yamane, K., Nishikawa, M., Hirooka, Y., Narita, Y., Kobayashi, T., Kakiuchi, M., Iwai, K., Iijima, M., 2022. Temperature tolerance threshold and mechanism of oxidative damage in the leaf of Coffea arabica 'Typica' under heat stress. Plant Prod. Sci. 25 (3), 337–349.